The Journal of Experimental Biology 213, 459-468

doi:10.1242/jeb.029363

Basolateral NBCe1 plays a rate-limiting role in transepithelial intestinal HCO_3^- secretion, contributing to marine fish osmoregulation

J. R. Taylor*, E. M. Mager and M. Grosell

Rosenstiel School of Marine and Atmospheric Science, University of Miami, Miami, FL, 33149-1098, USA

*Author for correspondence (jtaylor@rsmas.miami.edu)

Accepted 21 October 2009

SUMMARY

Although endogenous CO_2 hydration and serosal HCO_3^- are both known to contribute to the high rates of intestinal HCO_3^- secretion important to marine fish osmoregulation, the basolateral step by which transepithelial HCO_3^- secretion is accomplished has received little attention. Isolated intestine HCO_3^- secretion rates, transepithelial potential (TEP) and conductance were found to be dependent on serosal HCO_3^- concentration and sensitive to serosal DIDS. Elevated mucosal Cl^- concentration had the unexpected effect of reducing HCO_3^- secretion rates, but did not affect electrophysiology. These characteristics indicate basolateral limitation of intestinal HCO_3^- secretion in seawater gulf toadfish, *Opsanus beta*. The isolated intestine has a high affinity for serosal HCO_3^- in the physiological range (K_m=10.2 mmol l^{-1}), indicating a potential to efficiently fine-tune systemic acid–base balance. We have confirmed high levels of intestinal tract expression of a basolateral Na^+/HCO_3^- cotransporter of the electrogenic NBCe1 isoform in toadfish (tfNBCe1), which shows elevated expression following salinity challenge, indicating its importance in marine fish osmoregulation. When expressed in *Xenopus* oocytes, isolated tfNBCe1 has transport characteristics similar to those in the isolated tissue, including a similar affinity for HCO_3^- (K_m=8.5 mmol l^{-1}). Reported affinity constants of NBC1 for Na^+ are generally much lower than physiological Na^+ concentrations, suggesting that cotransporter activity is more likely to be modulated by HCO_3^- rather than Na^+ availability *in vivo*. These similar functional characteristics of isolated tfNBCe1 and the intact tissue suggest a role of this cotransporter in the high HCO_3^- secretion rates of the marine fish intestine.

Key words: anion exchange, SLC4, water absorption, carbonic anhydrase, acid–base balance.

INTRODUCTION

During the last decade, intestinal HCO_3^- secretion *via* apical Cl^-/HCO_3^- exchange has become recognized as an important component in the processing of seawater ingested to meet the osmoregulatory needs of marine fish (Wilson et al., 2002; Grosell, 2006; Marshall and Grosell, 2006). This anion exchange has been shown to contribute up to 70% of net Cl^- uptake and thereby water absorption by the marine teleost intestine (Grosell et al., 2005), counteracting diffusive water loss to the dehydrating seawater environment. While both endogenous and serosal sources are known to contribute HCO_3^- to apical anion exchange (Wilson et al., 2002; Grosell, 2006; Marshall and Grosell, 2006), the basolateral step of transepithelial HCO_3^- secretion in the marine fish intestine has received relatively little attention. In most species examined, the contribution of serosal HCO_3^- is likely to match or exceed that of endogenous CO_2 hydration (Grosell, 2006; Grosell and Genz, 2006) under *in vivo* conditions where serosal HCO_3^- concentrations range from 4 to 10 mmol l^{-1} (Wilson, 1999). This significant contribution makes the characterization of basolateral HCO_3^- transport essential to the understanding of marine fish osmoregulation.

Intestinal HCO_3^- secretion in marine fish occurs by a similar transport mechanism to that known in mammals. The function of HCO_3^- secretion as part of duodenal protection from gastric acid passing through the pyloric sphincter with chyme during the postprandial period is presumably common to those vertebrates relying on gastric acid secretion for digestion. However, intestinal HCO_3^- secretion in fish serves an additional role in contributing to osmoregulation. This difference between mammals and marine fish probably explains why intestinal HCO_3^- secretion in mammals occurs at highly varied rates (Hogan et al., 1994) and results in much lower intestinal fluid concentrations than seen in marine teleost fish. Early studies of mammalian intestinal transport found intestinal fluid HCO_3^- concentration in range of 6.4 to 18.2 mmol l^{-1}, and was always less than that of the serum (Herrin, 1935). Conversely, the osmoregulatory demands of marine fish lead to intestinal fluid HCO_3^- concentrations often approaching or even exceeding 100 mmol l^{-1} (Wilson et al., 2002), indicating high secretion rates against a HCO_3^- gradient. In addition to apical Cl^-/HCO_3^- exchange facilitating water absorption by contributing to Cl^- uptake (Grosell et al., 2005), these high concentrations of HCO_3^- lead to precipitation of $CaCO_3$ from the intestinal fluids (Smith, 1930; Walsh et al., 1991; Grosell, 2006). This carbonate precipitation is a phenomenon unique to osmoregulating marine fish and provides osmotic pressure depression in intestinal fluids (by as much as 70 mOsm), thereby enhancing the osmotic gradient for fluid absorption along the intestinal tract (Wilson et al., 2002; Wilson and Grosell, 2003; Marshall and Grosell, 2006).

Action by three distinct acid/base transporters has been proposed in both mammalian and piscine intestinal HCO_3^- secretion. In addition to apical anion exchange by a member of the SLC26 family (McMurtrie et al., 2004; Dorwart et al., 2008; Kurita et al., 2008), basolateral extrusion of H^+ produced during endogenous CO_2 hydration occurs in exchange for Na^+ in mammals [*via* Na^+/H^+ exchange, NHE (Hogan et al., 1994)], with this mechanism of Na^+-dependent H^+ extrusion characterized in one fish species [gulf toadfish (Grosell and Genz, 2006)]. Finally, a basolateral Na^+/HCO_3^- cotransporter (NBC) of the electrogenic, NBCe1 isoform has been

described in mammalian (Romero and Boron, 1999; Romero et al., 2004) and also recently in fish (Kurita et al., 2008) intestinal transepithelial HCO_3^- secretion. A comprehensive diagram of salt transport by the marine teleost intestine can be found in recent reviews (Grosell, 2006; Grosell et al., 2009a).

The implications of this high magnitude of intestinal base secretion for fish acid–base balance regulation have been largely overlooked. Elevated intestinal HCO_3^- secretion rates are suggested to be induced during the postprandial period (Taylor and Grosell, 2006) when many animals, including a limited number of fish species [an elasmobranch (Wood et al., 2005) and freshwater trout (Bucking and Wood, 2008; Cooper and Wilson, 2008)], have been shown to experience a metabolic alkalosis commonly referred to as alkaline tide (Niv and Fraser, 2002). Based on studies indicating the absence of an anticipated alkaline tide (Taylor et al., 2007) and an increase in intestinal HCO_3^- secretion (Taylor and Grosell, 2006) in postprandial euryhaline fish, we present the intestine as a potential site of metabolic alkalosis compensation *via* transepithelial HCO_3^- secretion. We hypothesize that NBC is present in the basolateral membrane of seawater-acclimated toadfish intestine and is important for transepithelial HCO_3^- transport. We also predict NBC to have altered expression in conditions requiring high intestinal HCO_3^- secretion rates, and thereby to possibly control the rate of HCO_3^- secretion by the marine fish intestine. Since a specific pharmacological NBC inhibitor is not available, we compared the functional characteristics of the toadfish NBC transporter expressed in *Xenopous* oocytes to those of the isolated marine fish intestine and provide evidence for an essential role of basolateral NBC in transepithelial HCO_3^- secretion by the marine fish intestine.

MATERIALS AND METHODS

Gulf toadfish (*Opsanus beta* Goode and Bean), were obtained by trawl from Biscayne Bay as by-catch by shrimp fishermen local to Miami, FL, USA, between March 2007 and October 2008. Within hours of capture, fish were transported to the wetlab facility at the Rosenstiel School of Marine and Atmospheric Science at the University of Miami, FL, USA and subjected to an ecto-parasite treatment (McDonald et al., 2003). Prior to experimentation, fish were maintained in the laboratory for a minimum of 2 weeks in aquaria with a constant flow of filtered, aerated seawater (32±1‰; parts per thousand) at 24±2°C from Bear Cut, FL, USA. These aquaria were equipped with PVC shelters to reduce stress and aggression among fish. Toadfish were fed chopped squid to satiation twice weekly until 72 h prior to experimentation, after which time food was withheld to ensure complete clearing of the gastrointestinal tract. All experimental procedures have been approved by our Institutional Animal Care and Use Committee under protocol 08–017.

In vitro HCO_3^- secretion by isolated intestinal tissue: electrophysiological measurements and pH-stat titration

To simultaneously investigate electrophysiological parameters and HCO_3^- secretion rates of isolated intestinal epithelia, Ussing chambers (Physiologic Instruments, San Diego, CA, USA) were set up in combination with pH-stat titration. A segment of the anterior intestine was excised from each experimental animal (toadfish ranging from 20 to100 g), cut open, and mounted onto a tissue holder (model P2413, Physiological Instruments) exposing 0.71 cm^2 of the isolated tissue and positioned between two half-chambers (model P2400; Physiological Instruments) containing 1.6 ml of the appropriate, pre-gassed, mucosal or serosal saline (Table 1). The saline in each half-chamber was continually mixed by airlift gassing with either O_2 or 0.3% CO_2 in O_2 (Table 1), and a constant temperature of 25°C was maintained by a thermostatic water bath. Current and voltage electrodes connected to amplifiers (model VCC600; Physiological Instruments) recorded the transepithelial potential (TEP) differences under current-clamp conditions at 0 μA, with 3-s, 50 μA pulses from the mucosal to the serosal side at 60-s intervals. These current-clamped conditions were maintained across all treatments. TEP measurements were logged on a personal computer using BIOPAC systems interface hardware and Acqknowledge software (version 3.8.1). TEP values are reported with a luminal reference of 0 mV. A pH electrode (model PHC4000.8, Radiometer, Copenhagen, Denmark) and microburette

Table 1. Composition of serosal and mucosal salines used in isolated tissue experiments

	Serosal				Mucosal	
Constituents	0 mmol l^{-1} HCO_3^-	5 mmol l^{-1} HCO_3^-	10 mmol l^{-1} HCO_3^-	20 mmol l^{-1} HCO_3^-	Mucosal	High Cl^- mucosal
NaCl, mmol l^{-1}	151	151	151	151	69	69
Choline-Cl, mmol l^{-1}						32
KCl, mmol l^{-1}	3	3	3	3	5	5
$MgCl_2$, mmol l^{-1}					22.5	22.5
$MgSO_4$, mmol l^{-1}	0.88	0.88	0.88	0.88	77.5	77.5
Na_2HPO_4, mmol l^{-1}	0.5	0.5	0.5	0.5		
KH_2PO_4, mmol l^{-1}	0.5	0.5	0.5	0.5		
$CaCl_2$, mmol l^{-1}	1	1	1	1	5	5
$NaHCO_3$, mmol l^{-1}	0	5	10	20		
Hepes						
Free acid, mmol l^{-1}	11	11	11	11		
Sodium salt, mmol l^{-1}	11	11	11	11		
Urea, mmol l^{-1}	4.5	4.5	4.5	4.5		
Glucose, mmol l^{-1}	5	5	5	5		
Osmolality, mosmol l^{-1}	355*	355*	355*	355*	355*	355**
pH	7.800‡	7.800‡	7.800‡	7.800‡	7.800†	7.800†
Gas	O_2	0.3% CO_2 in O_2	0.3% CO_2 in O_2	0.3% CO_2 in O_2	O_2	O_2

*Adjusted with mannitol to ensure transepithelial isosmotic conditions in all experiments.
**Adjusted with choline chloride rather than mannitol to ensure transepithelial isosmotic conditions in all experiments.
†pH 7.800 was maintained by pH-stat titration.
‡pH was adjusted with HCl under continuous gassing prior to experimentation to ensure isionic H^+ conditions during measurements.

tip were submersed in the luminal half-chamber and were connected to a pH-stat titration system (model TIM 854 or 856, Radiometer) grounded to the amplifier to allow for pH readings during current pulsing. The pH-stat titrations were performed on luminal salines at a physiological pH of 7.8 throughout all experiments (creating symmetrical pH conditions on either side of the epithelium), with pH values and rate of acid titrant (0.005 mol l^{-1} HCl) addition logged on personal computers using Titramaster software (versions 1.3 and 2.1). Titratable alkalinity, representing HCO_3^- secretion (Grosell and Genz, 2006), was calculated from the rate of titrant addition and its concentration. All experiments entailed an initial control period of 60 min with stable TEP and base secretion rates before manipulations were carried out as described below. The intestinal preparations from gulf toadfish are viable and stable for at least 5 h under these conditions (Grosell and Genz, 2006). Each preparation was allowed to stabilize (as determined from the titration curves) for approximately 30 min after application of each experimental saline before HCO_3^- secretion rates and electrophysiological parameters were averaged and reported for the remaining 30 min of exposure.

Affinity for serosal HCO_3^-

Affinity of the isolated gulf toadfish anterior intestine for serosal HCO_3^- was investigated using serosal salines varying in HCO_3^- concentration from 0 to 20 mmol l^{-1} (Table 1). Following a 60 min period during which HCO_3^- secretion rates were quantified under control mucosal and 20 mmol l^{-1} HCO_3^- serosal salines, the serosal saline was carefully removed from the half-chamber *via* PE60 tubing connected to a 5 ml syringe. The serosal half-chamber (including the serosal membrane of the epithelium) was rinsed twice and refilled with an equal volume of serosal saline containing 10 mmol l^{-1} HCO_3^-. An additional 60 min period was allowed for quantification of HCO_3^- secretion rates with 10 mmol l^{-1} serosal HCO_3^-, followed by identical treatments with serosal salines containing 5 and then 0 mmol l^{-1} HCO_3^-.

Limitation by mucosal Cl^- concentration

Upon finding evidence for saturation of intestinal HCO_3^- secretion rates at elevated serosal HCO_3^- concentrations, we investigated the possibility that overall epithelial secretion rates and specifically apical anion exchange may be limited by mucosal Cl^- concentrations when serosal HCO_3^- concentration is above *in vivo* concentrations. Following a 60 min period during which HCO_3^- secretion rates were quantified during exposure of the epithelium to control mucosal and 20 mmol l^{-1} HCO_3^- serosal salines, the control mucosal saline was removed as above and replaced with high-Cl^- mucosal saline (Table 1). Once the physiological pH of 7.8 was reached in the experimental mucosal saline, pH-stat titration data were recorded for 60 min after which control conditions were resumed for an additional 60 min by replacing the mucosal saline as described above.

Inhibition of HCO_3^- secretion by serosal DIDS application

Bicarbonate secretion rates by the isolated intestine were quantified before and after serosal application of 4,4′-diisothiocyanatostilbene-2,2′-disulfonic acid (DIDS; Sigma, St. Louis, MO, USA), which has been shown to inhibit both anion exchange and NBC (Romero et al., 1997). Prior to application, DIDS was dissolved in DMSO (Sigma) at a final concentration of less than <0.01%. DIDS was applied at a final concentration of 1 mmol l^{-1} in the serosal saline which in preliminary experiments was found to induce maximal inhibition (data not shown). Control experiments were carried out in presence of DMSO alone.

Molecular characterization of NBC

RNA isolation

For the initial identification and characterization of NBC in gulf toadfish, total RNA was extracted from anterior intestine tissue using RNA STAT-60 (Tel-Test, Friendswood, TX, USA). Briefly, tissue was homogenized in RNA STAT-60 (approx. 50–100 mg tissue per ml RNA STAT-60) using an IKA-Werke (Wilmington, NC, USA) Ultra-turrax T8 tissue homogenizer, and subjected to chloroform extraction and isopropanol precipitation. Precipitated RNA was washed with chilled 75% (v/v) ethanol and dissolved in nuclease-free water, and its concentration was measured spectrophotometrically at 260 nm. To remove any traces of genomic DNA, 10 μg from each sample was treated with DNase (Turbo DNA-free kit, Applied Biosystems/Ambion, Austin, TX, USA) followed by gel electrophoresis to confirm that RNA integrity was maintained.

Molecular cloning

cDNA was reverse transcribed from 1 μg poly(A) RNA using random hexamers and the SuperScript First-Strand Synthesis System (Invitrogen, Carlsbad, CA, USA) according to the manufacturer's instruction. Conserved regions of rainbow trout, zebrafish, salamander, rat and human NBC1 (NM 001124325.1, NM 001034984, AF001958, AF004017 and AF069510, respectively) were used to design three sets of primers (NBC1 1-3; Table 2) to amplify overlapping fragments of toadfish NBC from the cDNA template described above using AmpliTaq Gold polymerase (Applied Biosystems/Ambion). Assemblage of the resulting 2406 bp contig was later confirmed by alignment with the entire open reading frame (ORF) subsequently cloned by PCR for expression in *Xenopus* oocytes (see below). This contig was then used to design gene-

Table 2. Primer pairs used to amplify an initial (2406 bp) fragment of tfNBCe1 (NBC1 1-3), RACE gene-specific and nested gene-specific primers, those used to clone the entire open reading frame of NBC1, and qPCR primer pairs for tfNBCe1 and EF1α

	Forward primer sequence (5′→3′)	Reverse primer sequence (5′→3′)
NBC1 1	CACCAGACCAAGAAGTCCAAC	GRATGAAKGACATSAGHGTGA
NBC1 2	CATGCAGGGYGTGTTGGAGAG	ATGTGDGCRATGGAGATGAC
NBC1 3	CTTCATCTTCATYTAYGAYGC	CATCCAGGTARCTGAGATCDTGCTG
NBC1 5′ RACE GSP		GGGTGGTAAACAGCCTACTTGCACTGG
NBC1 3′ RACE GSP	ATGCTCTGGATCCTCAAATCCACCGTGG	
NBC1 5′ RACE NGSP		AGCGCAGGTTGGACTTCTTGGTCTGGTG
NBC1 3′ RACE NGSP	TTCTCCCAGCACGATCTCAGCTACCTGG	
NBC1 ORF	GATGGAAGATGAGGCGGTGTTGGAC	CCTTGTAGTAGCGGAGCTTCTCAGCACG
NBC1 qPCR	ACCAAAGTTTCTGGGTGTCAGAGAGCA	ACAGCACAGGCATAGGGATGAACTTTA
EF1α	AGGTCATCATCCTGAACCAC	GTTGTCCTCAAGCTTCTTGC

GSP, RACE gene-specific primers; NGSP, nested gene-specific primers; ORF, open reading frame.

specific and nested gene-specific primers (GSP and NGSP, respectively; Table 2) for rapid amplification of cDNA ends (RACE) to obtain full-length NBC sequences. Briefly, the SmartRACE cDNA synthesis kit (Clontech, Mountain View, CA, USA) was used to reverse transcribe 1 μg poly(A) RNA and amplify RACE-ready cDNA, which was subjected to touchdown PCR cycling conditions per the manufacturer's recommendations. A second round of amplification was carried out on diluted aliquots (1:100) of the initial amplifications using nested gene-specific primers (Table 2). Products were gel-purified, TA-cloned into the pCR 2.1 vector (Invitrogen) and sequenced. The full-length NBC sequence was confirmed by BLAST (National Center for Biotechnology Information, Bethesda, MD, USA) query as the electrogenic NBCe1 isoform, hereafter referred to as tfNBCe1 (accession no. FJ463158). Subsequently, the entire coding region of tfNBCe1 was cloned by PCR (Table 2) using the Advantage 2 (Clontech, Mountain View, CA, USA) high-fidelity enzyme mix and 5′ RACE-ready cDNA as template. Following TA cloning and sequence verification, the full-length ORF was subcloned into the *Eco*RI site of the pGH19 *Xenopus laevis* expression vector (kindly provided by Dr Gerhard Dahl, University of Miami Miller School of Medicine, Miami, FL, USA) using the LigaFast Rapid DNA Ligation System (Promega, Madison, WI, USA).

Real-time PCR

Tissue distribution of tfNBCe1 in gulf toadfish was initially quantified by real-time PCR under seawater control conditions. An acute salinity increase was then used to increase drinking rates (Marshall and Grosell, 2006) and thereby exploit mechanisms associated with this increased need for intestinal water absorption. tfNBCe1 expression was accordingly quantified in appropriate osmoregulatory tissues at 0, 6, 12, 24 and 96 h following acute salinity increase. Initially, eight fish (20–30 g) held in seawater aquaria as described above were given a lethal dose of MS-222 anaesthetic prior to severing the spinal cord. Esophagus, stomach, anterior intestine, mid intestine, posterior intestine, rectum, gill, kidney, muscle, liver, brain and spleen were obtained by dissection and immediately flash frozen in liquid nitrogen prior to transfer to a –80°C freezer.

From a batch of 40 additional toadfish (20–30 g) split between four 75-l aquaria receiving biofiltered, recirculated seawater, eight were sampled immediately (two individuals from each tank) for gill, anterior, mid, posterior intestine and rectum by dissection. The remaining 32 fish were maintained in their respective aquaria as the salinity was raised to 60 p.p.t. within a 5 min timeframe by the addition of a concentrated solution of Instant Ocean (Spectrum Brands, Inc). At 6, 12, 24 and 96 h post transfer to 60 p.p.t., eight fish per time point were sampled as above. From all tissues collected, RNA was extracted, purified and reverse transcribed as above. Quantitative PCR (Mx4000, Stratagene, La Jolla, CA, USA) was used to measure tfNBCe1 mRNA expression using primers listed in Table 2 with SYBR green (Sigma) as the reporter dye. Cycling parameters were as follows: 95°C for 30 s, 55°C for 30 s and 72°C for 1 min. Calculations were performed based on the $\Delta\Delta C_T$ approach (Livak and Schmittgen, 2001) using elongation factor 1α (EF1α) for normalization of template concentration. Owing to the absence of an available toadfish-specific sequence for EF1α, primers were designed from highly conserved regions across multiple teleost species. All PCR product specificities were confirmed by sequencing and the production of single, distinct melting peaks following amplification. Relative tfNBCe1 expression was calculated for each exposure group such that the tissue expressing the lowest quantity of tfNBCe1 (i.e. kidney in seawater control conditions, and gill under increased salinity conditions) was assigned an expression value of one.

Expression of tfNBCe1 in *Xenopus* oocytes

Oocyte preparation

Oocytes were prepared for RNA injections as described previously (Dahl, 1992). After being washed thoroughly with regular oocyte ringer (OR2; Table 3), oocytes devoid of follicle cells and having uniform pigmentation were selected and stored in OR2 at 17°C. mRNA was transcribed *in vitro* by T7 RNA polymerase from 1 μg of *Xho*I-linearized plasmid DNA using the mMESSAGEmMACHINE kit (Applied Biosystems/Ambion). Oocytes were injected with 50 nl of water or 1 μg μl^{-1} cRNA using a Nanoliter 2000 injector (World Precision Instruments, Sarasota, FL, USA). Oocytes were incubated at 17°C in regular (pyruvate-free) ND96 medium (Table 3) containing antibiotics (penicillin, 10,000 i.u. ml^{-1}; streptomycin, 10 mg ml^{-1}) until Na^+ flux and electrophysiology experiments commenced 3 and 4 days after injection, respectively, as described below.

^{22}Na flux

On the third day following injection, control (H_2O–) and tfNBCe1 RNA-injected oocytes were selected in groups of 10, rinsed briefly in the appropriate antibiotic-free experimental ND96 saline (Table 3) containing the NHE and NKCC inhibitors amiloride (100 μmol l^{-1}; Sigma) and bumetanide (10 μmol l^{-1}; Sigma), respectively. Amiloride and bumetanide were added to all experimental salines to inhibit any intrinsic NHE and NKCC activity by oocytes (Dascal, 1987). Groups of 10 oocytes were then placed in conical-bottomed wells of a 96-well plate, each containing 150 μl of the experimental saline (Table 3) to which 7.5 μCi ^{22}Na (Amersham Biosciences, Sweden) per well had been added. Initial flux samples (10 μl) were taken for gamma counting so that any dilution of the experimental medium during oocyte addition could be accounted for. Following preliminary experiments revealing possible saturation of ^{22}Na uptake by oocytes after 90–120 min (data not shown), 75 min was identified as the most appropriate flux time and was used for all subsequent experiments. At the end of the flux period, all 10 oocytes were carefully removed from the well using a Pasteur pipette and subjected to three serial rinses in regular antibiotic-, drug- and HCO_3^--free ND96 saline. Following the final rinse, oocytes were examined under a dissecting microscope for damage to the plasma membrane. Undamaged oocytes (generally 80–90%) were selected for gamma counting. A final flux sample (10 μl) was also taken from each well for gamma counting. Samples were analyzed for ^{22}Na activity (Packard Cobra II Auto-Gamma, Meriden, Connecticut, USA), Na^+ concentration was measured by flame atomic absorption spectrophotometry (Varian SpectrAA220, Mulgrave, Victoria, Australia), and Na^+ uptake was calculated from the radioactivity and specific activity measurements. These experiments were designed to complement isolated tissue measurements by allowing us to quantify affinity of the isolated tfNBCe1 for HCO_3^- during exposure to 0, 5, 10 and 20 mmol l^{-1} HCO_3^-.

tfNBCe1 transmembrane topology prediction

The amino acid sequence of tfNBCe1 was used to predict the transmembrane topology of this protein using hydropathy plots based on Kyte and Doolittle (Kyte and Doolittle, 1982), and models generated by TMPred (hosted by the Swiss Institute of Bioinformatics) and ConPredII (hosted by Hirosaki University, Hirosaki, Japan; and Tohoku University, Sendai, Japan).

Table 3. Composition of solutions used in oocyte ^{22}Na flux experiments

		ND96			
	OR2	0 mmol l^{-1} HCO_3^-	5 mmol l^{-1} HCO_3^-	10 mmol l^{-1} HCO_3^-	20 mmol l^{-1} HCO_3^-
NaCl, mmol l^{-1}	82.5	99	99	99	99
Choline-Cl, mmol l^{-1}					
KCl, mmol l^{-1}	2.5	2	2	2	2
$MgCl_2$, mmol l^{-1}	1	1	1	1	1
$CaCl_2$, mmol l^{-1}	1	1.8	1.8	1.8	1.8
$NaHCO_3$, mmol l^{-1}		0	5	10	20
$NaHPO_4$, mmol l^{-1}	5				
Hepes (Free acid), mmol l^{-1}	5	1	1	1	1
Osmolality, mosmol l^{-1}		240*	240*	240*	240
pH†	7.40	7.40	7.40	7.40	7.40
$NaHPO_4$, mmol l^{-1}	5				
Hepes (Free acid), mmol l^{-1}	5	1	1	1	1
Osmolality, mosmol l^{-1}		240*	240*	240*	240
pH†	7.40	7.40	7.40	7.40	7.40
NaCl, mmol l^{-1}	82.5	99	99	99	99
Choline-Cl, mmol l^{-1}					
KCl, mmol l^{-1}	2.5	2	2	2	2
$MgCl_2$, mmol l^{-1}	1	1	1	1	1
$CaCl_2$, mmol l^{-1}	1	1.8	1.8	1.8	1.8
$NaHCO_3$, mmol l^{-1}		0	5	10	20
$NaHPO_4$, mmol l^{-1}	5				
Hepes (Free acid), mmol l^{-1}	5	1	1	1	1
Osmolality, mosmol l^{-1}		240*	240*	240*	240
pH†	7.40	7.40	7.40	7.40	7.40

*Adjusted with mannitol to ensure equal osmotic gradients in all experiments.
†pH adjusted with appropriate amounts of HCl or NaOH to pH 7.40 prior to experimentation.

Statistics

Data are presented as means ± s.e.m. For all isolated tissue measurements, repeated measures ANOVA or paired *t*-tests were used to determine statistically significant differences from control conditions. Significant expression of tfNBCe1 in tissues from seawater-acclimated toadfish was determined by ANOVA comparison of normalized tfNBCe1 expression in each tissue to that of the lowest-expressing tissue, the kidney (normalized tfNBCe1 expression=1). In measurements of tfNBCe1 expression following salinity transfer, expression in each tissue sample was quantified by comparison with the lowest-expressing sample, gill 0 h post-transfer (normalized tfNBCe1 expression=1). Between-timepoint comparisons were made within each tissue group using one-way ANOVA. Significant changes in oocyte Na^+ uptake from that of controls were also determined by one-way ANOVA. The Student–Newman–Keuls test was used for all multiple comparisons as appropriate, and statistical significance was given at $P<0.05$ in all cases. Hyperbolic curves of equation $f=ax/(b+x)$ or $f=y_0+ax/(b+x)$ were fit to relevant data sets using SigmaPlot 8.0, with $a=V_{max}$ and $b=K_m$.

RESULTS

Isolated intestinal tissue transport characteristics

Affinity for serosal HCO_3^-

A plot of HCO_3^- secretion rate by the isolated toadfish anterior intestine as a function of serosal HCO_3^- concentration is shown in Fig. 1. A hyperbolic curve was fit (R=0.70) to these data and maximal HCO_3^- secretion rates (V_{max}) of 1.26 μmol cm^{-2} h^{-1} were calculated. Subtraction of HCO_3^- secretion rates under HCO_3^--free conditions (Table 4) suggests 0.92 μmol cm^{-2} h^{-1} (>70%) of this V_{max} is conferred by transepithelial rather than endogenous HCO_3^- secretion, during the constant metabolic rates expected under these experimental conditions. For calculation of the basolateral HCO_3^- affinity constant K_m, secretion rates during exposure to 0 mmol l^{-1} serosal HCO_3^- were subtracted from all measurements such that the calculated K_m of 10.2 mmol l^{-1} HCO_3^- is exclusively a measure of affinity for serosal HCO_3^- without interference by endogenous CO_2-mediated HCO_3^- secretion. Depressed HCO_3^- secretion rates under decreasing serosal [HCO_3^-] were accompanied by significant reductions in both TEP and conductance (Table 4). Changes in conductance were notably modest compared with those seen for TEP and probably reflect other transport pathways.

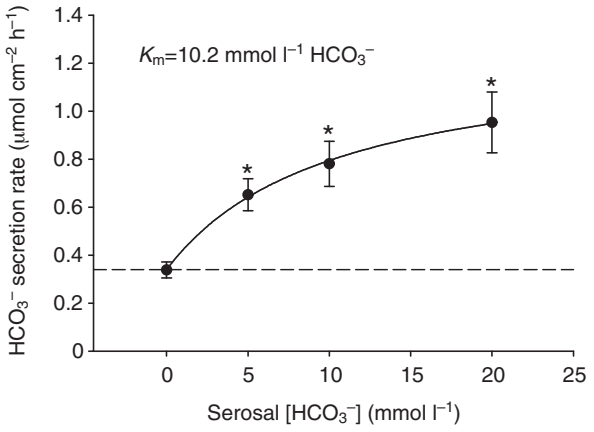

Fig. 1. The isolated toadfish anterior intestine (n=8) shows saturation of luminal HCO_3^- secretion rates with increasing serosal [HCO_3^-]. Asterisks denote a significant increase in HCO_3^- secretion rate from that at 0 mmol l^{-1} serosal HCO_3^- (0.34 μmol cm^{-2} h^{-1}; dashed line). Maximal HCO_3^- secretion rate (V_{max}) by the entire system (both serosal and endogenous sources of HCO_3^-) was calculated to be 0.92 μmol cm^{-2} h^{-1}.

Table 4. Measurements made on toadfish isolated anterior intestine

	HCO_3^- secretion ($\mu mol\,cm^{-2}\,h^{-1}$)	TEP (mV)	Conductance (μSi)
Affinity for serosal HCO_3^- (n=8)			
0 mmol l^{-1} serosal HCO_3^-	0.34±0.03	–14.23±1.90	11.01±0.44
5 mmol l^{-1} serosal HCO_3^-	0.65±0.07*	–16.86±1.75*	11.55±0.40*
10 mmol l^{-1} serosal HCO_3^-	0.78±0.09*	–19.18±1.54*	11.57±0.33*
20 mmol l^{-1} serosal HCO_3^-	0.95±0.13*	–22.66±0.77*	11.63±0.40*
Effects of mucosal $[Cl^-]$ (n=6)			
Control mucosal $[Cl^-]$ (treatment 1)	1.19±0.06	–24.49±1.56	12.25±0.29
High mucosal $[Cl^-]$ (treatment 2)	0.81±0.05*	–24.50±1.31	12.50±0.30
Control mucosal $[Cl^-]$ (treatment 3)	0.86±0.10*	–24.70±2.40	12.71±0.77
Serosal DIDS application (n=6)			
Control	1.25±0.11	–23.65±1.65	11.76±0.35
DIDS	0.78±0.07*	–19.41±2.64*	10.11±0.64*
Serosal DMSO sham application (n=6)			
Control	1.29±0.09	–23.72±3.36	12.37±0.23
DMSO	1.08±0.08	–21.33±4.46	12.64±0.22

Values are means ± s.e.m.; *statistically significant difference from control.
TEP, transepithelial potential.

Limitation by mucosal Cl^- concentration

To further investigate the saturation of HCO_3^- secretion rates with increasing serosal HCO_3^- concentration, experiments using a range of serosal Na^+ concentration were attempted; however, saline chemistry limitations unfortunately prevent the use of low serosal Na^+ concentration without simultaneously altering Cl^- concentration. Thus experiments alternating normal and high Cl^- concentration mucosal salines were undertaken to ensure that the saturation of HCO_3^- secretion induced by increased serosal HCO_3^- concentration was in fact due to basolateral limitation rather than limitation of apical Cl^-/HCO_3^- exchange by mucosal Cl^- substrate. In the case of apical anion exchange limitation by mucosal Cl^- substrate, increasing the mucosal Cl^- concentration would be expected to increase the HCO_3^- secretion rates of the isolated tissue. However, our data show a significant and irreversible *decrease* in HCO_3^- secretion under high mucosal Cl^- concentration as compared with rates under normal mucosal Cl^- concentration (Table 4). Electrophysiological data show no significant changes in either TEP or conductance under high mucosal Cl^- concentration (Table 4).

Serosal DIDS application

Serosal application of the NBC and anion exchange inhibitor DIDS significantly decreased HCO_3^- secretion by the isolated tissue under 20 mmol l^{-1} serosal HCO_3^- from 1.25±0.11 $\mu mol\,cm^{-2}\,h^{-1}$ to 0.78±0.07 $\mu mol\,cm^{-2}\,h^{-1}$. This incomplete inhibition by DIDs resulted, at least in part, from the continuation of endogenous CO_2 production during serosal DIDs application. Likewise, TEP and conductance are both significantly inhibited in the presence of serosal DIDS (Table 4), albeit to a relatively smaller degree than HCO_3^- secretion rates because of to their dependence on processes other than HCO_3^- secretion (i.e. Na^+/K^+-ATPase).

tfNBCe1 mRNA expression

tfNBCe1 is most highly expressed along the intestinal tract of seawater-acclimated gulf toadfish, with the highest prevalence in the anterior intestinal tissue and decreasing amounts sequentially in posterior segments (Fig. 2). Significant tfNBCe1 expression was also measured in the brain (Fig. 2). Acute salinity increase allowed us to further investigate the role of tfNBCe1 in salt and water balance of toadfish. Based on their osmoregulatory importance, the intestinal tract and gill were the focus of tissue sampling following acute salinity challenge. A trend towards increased tfNBCe1 expression was seen in all intestinal tract tissues, and appeared to peak between the 6 and 24 h post-transfer period with increases ranging from 20 to nearly 300%. These increases in expression reached statistical significance only for the middle intestine (Fig. 3). Gill expression of tfNBCe1 remained stable relative to control levels during these time points, but was significantly elevated 96 h post-transfer.

Isolated tfNBCe1 transport characteristics

tfNBCe1 expression in *Xenopus* oocytes was indicated by significantly higher ^{22}Na uptake (Fig. 4A) than that by water-injected controls. In addition to the results described below, pharmacological inhibition of NBC in oocytes was attempted but unfortunately the DMSO vector used to dissolve DIDS proved too caustic to the oocyte membrane to yield reliable results (data not shown).

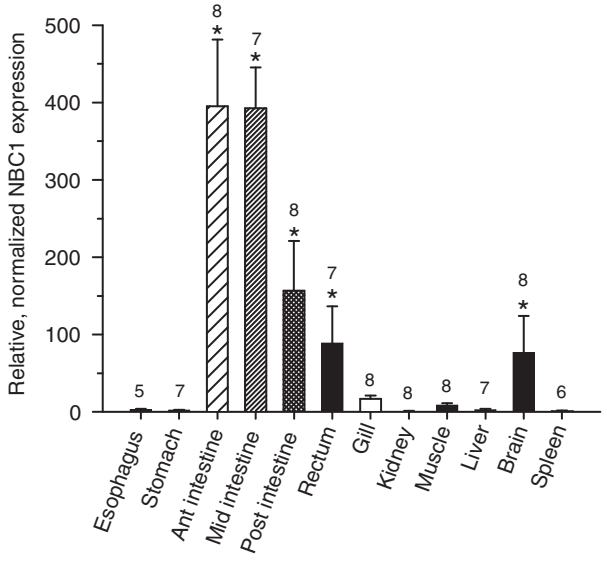

Fig. 2. Tissue distribution of tfNBCe1 mRNA expression in toadfish acclimated to seawater (n=6–8 for each tissue), normalized using the EF1α housekeeping gene and scaled relative to the tissue of lowest tfNBCe1 expression (kidney), which was assigned an expression value of one. Asterisks indicate tissues expressing tfNBCe1 to a significantly greater level than the kidney.

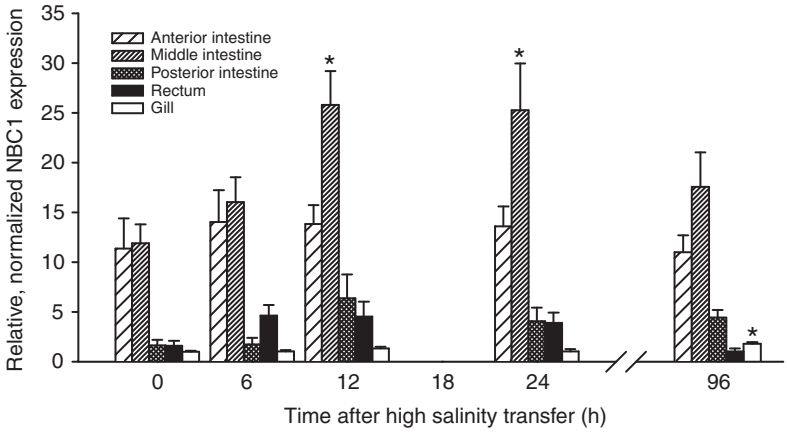

Fig. 3. tfNBCe1 mRNA expression in toadfish intestine, rectum and gill following acute transfer from seawater (35 p.p.t.) to 60 p.p.t. seawater, normalized using the EF1α housekeeping gene and scaled relative to the tissue of lowest NBC1 expression (gill 0 h post-transfer) which was assigned an expression value of one. Asterisks indicate significant increases in tfNBCe1 expression from 0 h levels. *N*=6–8 for each tissue. *N*=8 for each tissue at each timepoint, with the exception of 96 h rectum samples (*N*=7).

Affinity for HCO_3^-

The tfNBCe1 as expressed in *Xenopus* oocytes displayed affinity for HCO_3^- at a similar level to that of the isolated toadfish intestinal tissue. Increasing the HCO_3^- concentration of the flux medium from 0 to 5, 10 and 20 mmol l^{-1} HCO_3^- resulted in saturation of Na^+ uptake by tfNBCe1-expressing oocytes (Fig. 4B). Once counts were normalized to zero ^{22}Na uptake by oocytes fluxed in medium containing 0 mmol l^{-1} HCO_3^-, a hyperbolic curve was fitted (*R*=0.70) to these data with K_m=8.5 mmol l^{-1} HCO_3^-. These calculations were made assuming all Na^+/HCO_3^- cotransport occurred as uptake, with no interfering Na^+ efflux. This assumption was made based on the Na^+ reversal potential of approx. +55 mV under the experimental conditions.

Topology prediction

In order to draw more direct comparisons of tfNBCe1 with other known NBCe1 proteins with respect to both structure and possible function, we have predicted the topology of this protein. The structure of tfNBCe1 was predicted based on the 1,071 amino acid sequence including 12 transmembrane-spanning domains, with amino and carboxyl termini predicted to be cytosolic (Fig. 5). This structure prediction closely resembles those of other known NBCe1 proteins which is not surprising considering the strong amino acid sequence similarity between vertebrate NBCe1 proteins. A number of putative binding domains have been identified (Fig. 5) based on those characterized in other NBCe1 proteins and are discussed below with respect to their possible implications for protein function.

DISCUSSION

Our comparison of isolated toadfish intestine characteristics to those of isolated tfNBCe1 provides strong support for the involvement of NBCe1 in intestinal base secretion for marine osmoregulation. This role is supported by elevated mRNA expression of NBCe1 in the marine toadfish (present study) and the euryhaline pufferfish (Kurita et al., 2008) in response to elevated salinity.

We have shown that serosal HCO_3^- contributes significantly to HCO_3^- secretion by the isolated toadfish intestine under *in vivo*-like conditions of 4–10 mmol l^{-1} plasma HCO_3^- concentration (Wilson, 1999). At plasma HCO_3^- concentrations of 7 mmol l^{-1}, an estimated 48% of HCO_3^- secretion can be accounted for by endogenous CO_2 (Fig. 1), in agreement with findings by Grosell and Genz (Grosell and Genz, 2006) that 56% of isolated toadfish intestine HCO_3^- secretion could be explained by endogenous CO_2 at 5 mmol l^{-1} serosal HCO_3^- concentration. The high affinity of the basolaterally limited, isolated intestine for serosal HCO_3^- in the physiological range (Fig. 1) suggests its potential to efficiently fine-tune systemic acid–base balance by transepithelial intestinal HCO_3^- secretion and subsequent excretion in the rectal fluid. In addition to identifying this prospective role of transepithelial intestinal HCO_3^- secretion in plasma HCO_3^- regulation, our findings in

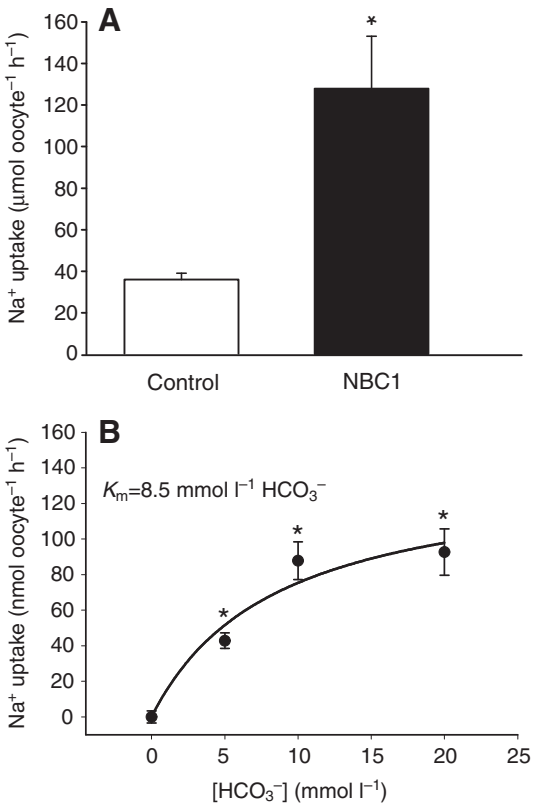

Fig. 4. (A) Expression of tfNBCe1 in *Xenopus* oocytes is indicated by significantly higher Na^+ uptake in tfNBCe1 RNA-injected *versus* H_2O-injected control oocytes during exposure to 10 mmol l^{-1} HCO_3^-. (B) Affinity of tfNBCe1 for HCO_3^- was determined by measuring Na^+ uptake in tfNBCe1-expressing oocytes exposed to varying HCO_3^- concentrations (*n*=18–20 oocytes at each [HCO_3^-]). Uptake has been adjusted for H_2O-injected controls and also such that background ^{22}Na uptake observed from HCO_3^--free saline has been subtracted from all values. A hyperbolic regression was used to calculate the affinity of tfNBCe1 for HCO_3^- as described in the text. Asterisks denote a significant increase in Na^+ uptake from oocytes exposed to HCO_3^--free saline (i.e. zero).

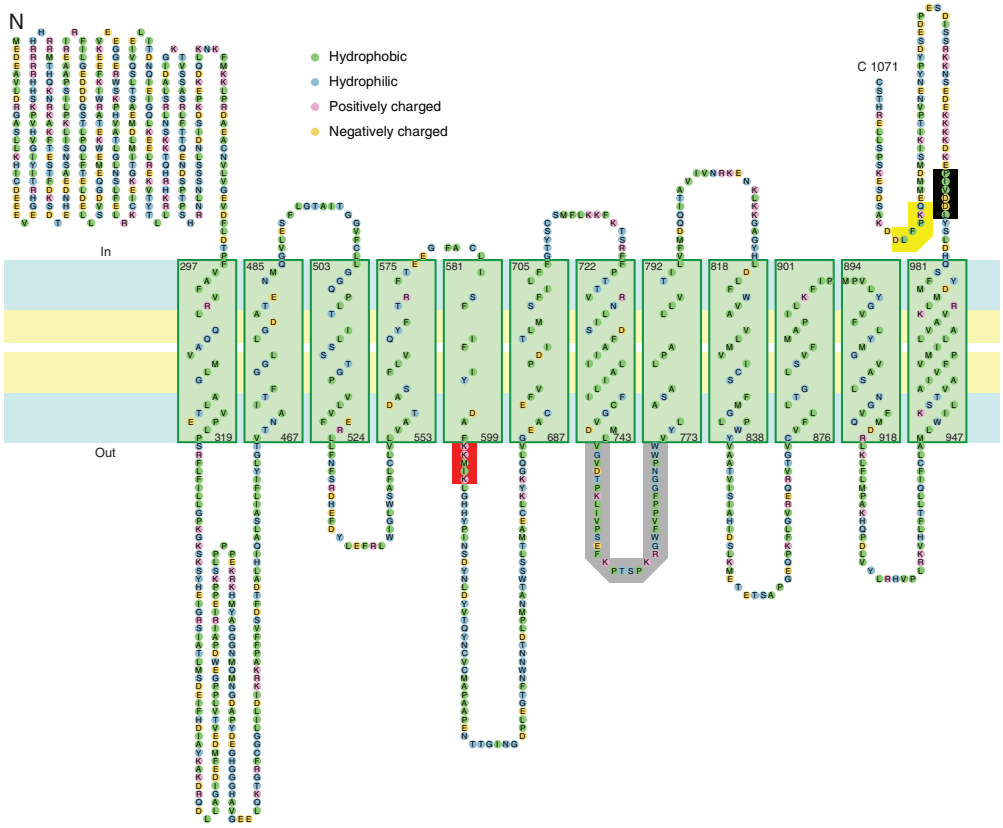

Fig. 5. Putative membrane topology of tfNBCe1 (FJ463158) with amino acids color coded based on the scheme of ConPredII (Japan). Putative DIDS and CAII-binding and basolateral targeting motifs are indicated by red, black and yellow shaded areas, respectively. The fourth extracellular loop (shaded gray) has been suggested to interact with CAIV (Alvarez et al., 2003). Putative transmembrane domains are indicated by vertical rectangles shaded light green.

toadfish are consistent with data from other species including trout (Grosell et al., 2007) and pufferfish (Kurita et al., 2008), suggesting that transepithelial HCO_3^- secretion is an important and universal feature of marine fish osmoregulation.

We have verified expression of the Na^+/HCO_3^- cotransporter, tfNBCe1, along the intestinal tract of seawater toadfish (Fig. 2) as a means by which this transepithelial HCO_3^- secretion is accomplished. Transiently increased tfNBCe1 expression following acute salinity increase (Fig. 3) supports recent findings by Kurita et al. (Kurita et al., 2008) showing elevated intestinal NBCe1 expression in pufferfish in response to elevated salinity, and underscores the importance of transepithelial HCO_3^- secretion, facilitated by basolateral tfNBCe1, in marine fish osmoregulation. Additionally, our results indicate that the scope for adjustment of intestinal HCO_3^- secretion rates by shifting serosal HCO_3^- availability is quite large. Despite the high levels of tfNBCe1 in both the anterior and middle intestine under control conditions (Fig. 2), salinity challenge reveals a shift towards higher expression of tfNBCe1 in the middle intestinal tissue (Fig. 3). The importance of anterior intestinal HCO_3^- secretion to chyme neutralization during digestion and the dominant role for this intestinal segment in salt and water absorption under normal seawater conditions (Grosell and Taylor, 2007) may be the basis for its more consistent high expression. However, more posterior segments of the intestinal tract appear to have a greater scope for increasing tfNBCe1 expression to maintain homeostasis during further osmoregulatory challenge.

Serosal HCO_3^- availability is altered by a number of physiological disturbances including postprandial metabolic alkalosis, commonly referred to as the alkaline tide (Niv and Fraser, 2002), during which fish can experience HCO_3^- concentrations up to approximately 12 mmol l^{-1} (Bucking and Wood, 2008). At these high levels, serosal HCO_3^- has the potential to contribute nearly 60% to intestinal HCO_3^- secretion (Fig. 1), assuming constant metabolic rate of the intestinal tissue. However, postprandial alkaline tide is accompanied by specific dynamic action (SDA) which in fishes accounts for an approximate 136% increase in whole-animal metabolic rates (Secor, 2008). Notably, organ-specific metabolic rate increases can be even more substantial (Secor, 2008) and may account for some or all of the elevated intestinal HCO_3^- secretion noted by Taylor and Grosell (Taylor and Grosell, 2006) in postprandial toadfish. These postprandial changes in whole-animal, and more specifically, intestinal tissue CO_2 production rates must be quantified for a more accurate assessment of the contribution of serosal HCO_3^- to intestinal HCO_3^- secretion and resulting implications for postprandial acid–base balance regulation. However, secretion of HCO_3^- derived from endogenous CO_2 will also result in an equimolar H^+ extrusion from the cell (Grosell, 2006; Grosell and Genz, 2006; Grosell et al., 2007; Grosell and Taylor, 2007; Grosell et al., 2009a; Grosell et al., 2009b) which should be investigated in more detail to determine its polarity and implications for regulation of acid–base balance.

Our experiments using isolated intestinal tissue indicate basolateral limitation of intestinal HCO_3^- secretion by an electrogenic mechanism. The dependence of HCO_3^- secretion rate, TEP and conductance on serosal HCO_3^- concentration (Fig. 1) suggests both basolateral limitation and electrogenicity, while the lack of HCO_3^- secretion stimulation under elevated mucosal Cl^- concentrations (Table 4) provides additional evidence against apical

limitation. A crucial role of the electrogenic tfNBCe1 in intestinal HCO_3^- secretion is supported by transporter characteristics that very closely match the basolaterally limited HCO_3^--transporting ability of the isolated intestine. The affinity of isolated tfNBCe1 for HCO_3^- (Fig. 4B) is analogous to that of the isolated intestine tissue (Fig. 1), with K_m very closely approximating reported plasma HCO_3^- concentration under normal (Wilson, 1999) and alkaline tide (Bucking and Wood, 2008) circumstances. The seemingly counterintuitive decrease in isolated intestinal tissue HCO_3^- secretion rates under elevated mucosal [Cl^-] supports previous suggestions that NaCl absorption is dominated by NaCl and NKCC cotransport mechanisms under relatively high luminal NaCl concentrations, whereas Cl^-/HCO_3^- gains importance when luminal substrates are limited to concentrations found *in vivo* (Grosell and Taylor, 2007). Meanwhile, reported K_m values of NBC1 for Na^+ (Jentsch et al., 1985; Sciortino and Romero, 1999; Horita et al., 2005; McAlear et al., 2006) are generally less than a quarter of the approx. 150 mmol l^{-1} Na^+ normal to teleost plasma. This suggests that cotransport by tfNBCe1 is more likely to be limited by serosal HCO_3^- availability under physiological conditions.

A sizeable body of literature pertaining to structure–function relationships within the HCO_3^- transporting protein superfamily (McMurtrie et al., 2004; Romero et al., 2004; Dorwart et al., 2008) has allowed us to make several correlations between our characterization of transepithelial HCO_3^- secretion and structural features predicted for tfNBCe1. First, a basolateral targeting motif with amino acid sequence QQPFLS has been identified in the cytoplasmic tail of mammalian kidney NBC1 (Li et al., 2007). Following a series of mutations the authors proposed the FL motif to be essential for the targeting of NBC1 to the basolateral membrane. The cytoplasmic tail of tfNBCe1 contains a similar amino acid motif at positions 1047–1052 (QKPFLD; Fig. 5), which notably contains the crucial FL motif. To confirm basolateral localization, immunohistochemistry was attempted using the mefugu NBCe1 antibody generously provided by Dr Hirose and co-workers (Kurita et al., 2008); however, this antibody was shown by western blot to lack specificity for NBC1 in toadfish intestine (data not shown). Second, as noted previously, the pharmacological inhibitor DIDS is not specific for NBC, but also inhibits anion exchange. This is due to a homologous positively charged motif with several conserved amino acids between the two protein families, with the sequence KKMIK playing an important role in both reversible and irreversible DIDS blockade of NBCe1 (Lu and Boron, 2007). This DIDS-binding motif is conserved at positions 600–604 at the extracellular end of TM5 in tfNBCe1 (Fig. 5), as predicted in human NBCe1 (Lu and Boron, 2007), suggesting tfNBCe1 is a candidate target for the inhibition of HCO_3^- secretion by the isolated tissue during serosal DIDS application (Table 4). Third and finally, a number of amino acid residues that are conserved in tfNBCe1 have been implicated in various metabolon hypotheses in mammalian systems (McMurtrie et al., 2004). Interaction of NBCe1 with CAIV is thought to occur in the fourth extracellular loop as suggested by Alvarez et al. (Alvarez et al., 2003), and with CAII at one or more acidic binding domains in the carboxyl-terminus (Sterling et al., 2001). In the case of marine fish intestinal HCO_3^- secretion, the cytoplasmic CAc (equivalent to CAII) isoform is also important in endogenous CO_2 hydration (McMurtrie et al., 2004; Grosell et al., 2007). Additionally, a mechanism has been proposed that involves CO_2 recirculation *via* apical anion exchange and subsequent dehydration of luminal HCO_3^- by protons supplied by apical H^+-ATPase and/or NHE and facilitated by extracellular, apically bound CAIV (Grosell et al., 2007; Grosell et al., 2009a; Grosell et al., 2009b). A similar model by which serosal CO_2 is pulled to basolateral NBC1, hydrated to HCO_3^- by extracellularly bound CAIV and 'drawn' through the cotransporter by intracellularly bound CAII dehydration has been proposed by Alvarez et al. (Alvarez et al., 2003). Together these proposed putative metabolon systems may explain the noteworthy efficiency of marine fish transepithelial HCO_3^- secretion including the high affinity of both the isolated tissue and isolated tfNBCe1 for serosal HCO_3^- (Fig. 1 and Fig. 4B). Modulation of the NBC1–CAII interaction has been suggested as a mode of NBC1 regulation (Gross et al., 2002), although this idea has been disputed by several recent studies (Lu et al., 2006; Piermarini et al., 2007). Given the efficiency of transepithelial HCO_3^- transport in the marine fish intestine, we suggest this model may be ideally suited for further evaluation of physical and functional interactions within the proposed metabolons.

Using a suite of complementary methods, we have presented evidence that basolateral tfNBCe1 is a rate-limiting component of intestinal HCO_3^- secretion in seawater-acclimated gulf toadfish with the potential to fine-tune plasma HCO_3^- concentration. The affinities of the isolated tfNBCe1 and the basolaterally limited epithelium for HCO_3^- are high and similar. The amino acid sequence of tfNBCe1 contains motifs specific for basolateral targeting and DIDS binding which is in agreement with our intact tissue experiments. These structure–function relationships combined with the high HCO_3^- secretion rates of marine teleost intestinal epithelia potentially arising from physical associations of tfNBCe1 with intracellular CAII and extracellular CAIV remain a fruitful model for study of tubular secretion of HCO_3^- in vertebrates. The efficiency of tfNBCe1 in transepithelial intestinal HCO_3^- secretion may also have implications for plasma HCO_3^- regulation, particularly for base excretion during the postprandial period (Taylor and Grosell, 2009). Exploring the transport characteristics of tfNBCe1 has provided support for this idea, but quantification of intestinal tissue-specific dynamic action concomitantly with HCO_3^- secretion (Taylor and Grosell, 2009) will allow more specific deductions to be made.

ACKNOWLEDGEMENTS

We thank Jimbo's and Ray Hurley, Miami, FL, USA, for supplying us with toadfish; Dr Gerhard Dahl and his group at the University of Miami Miller Medical School, Miami, FL, USA, for providing *Xenopus* oocytes, expression vector, and expertise; and Drs S. Hirose, M. D. McDonald, M. Schmale, and J. M. Wilson for providing us with immunohistochemistry materials and guidance. We also thank a particularly helpful reviewer for valuable insights during the peer review process. J.R.T. is supported by a University of Miami teaching assistantship and E.M.M. by an EPA STAR fellowship. The present study was supported by an NSF award (IOB 0718460) to M.G.

REFERENCES

Alvarez, B. V., Loiselle, F. B., Supuran, C. T., Schwartz, G. J. and Casey, J. R. (2003). Direct extracellular interaction between carbonic anhydrase IV and the human NBC1 sodium/bicarbonate co-transporter. *Biochemistry* **42**, 12321-12329.

Bucking, C. and Wood, C. M. (2008). The alkaline tide and ammonia excretion after voluntary feeding in freshwater rainbow trout. *J. Exp. Biol.* **211**, 2533-2541.

Cooper, C. A. and Wilson, R. W. (2008). Post-prandial alkaline tide in freshwater rainbow trout: effects of meal anticipation on recovery from acid-base and ion regulatory disturbances. *J. Exp. Biol.* **211**, 2542-2550.

Dahl, G. (1992). The *Xenopus* oocyte cell-cell channel assay for functional analysis of gap junction proteins. In *Cell–Cell Interactions: A Practical Approach* (ed. B. Stevenson, W. Gallin and D. Paul), pp. 143-165. New York, NY: Oxford University Press.

Dascal, N. (1987). The use of *Xenopus* oocytes for the study of ion channels. *CRC Crit. Rev. Biochem.* **22**, 317-387.

Dorwart, M. R., Shcheynikov, N., Yang, D. and Muallem, S. (2008). The Solute Carrier 26 family of proteins in epithelial ion transport. *Physiology* **23**, 104-114.

Grosell, M. (2006). Review: Intestinal anion exchange in marine fish osmoregulation. *J. Exp. Biol.* **209**, 2813-2827.

Grosell, M. and Genz, J. (2006). Ouabain sensitive bicarbonate secretion and acidic fluid absorption by the marine teleost intestine play a role in osmoregulation. *Am. J. Phys. Regul. Physiol.* **291**, R1145-R1156.

Grosell, M. and Taylor, J. R. (2007). Intestinal anion exchange in teleost water balance. *Comp. Biochem. Physiol.* **148A**, 14-22.

Grosell, M., Wood, C. M., Wilson, R. W., Bury, N. R., Hogstrand, C., Rankin, C. and Jensen, F. B. (2005). Active bicarbonate secretion plays a role in chloride and water absorption of the European flounder intestine. *Am. J. Physiol.* **288**, R936-R946.

Grosell, M., Gilmour, K. M. and Perry, S. F. (2007). Intestinal carbonic anhydrase, bicarbonate, and proton carriers play a role in the acclimation of rainbow trout to seawater. *Am. J. Physiol. Regul. Integr. Comp. Physiol.* **293**, R2099-R2111.

Grosell, M., Genz, J., Taylor, J. R., Perry, S. F. and Gilmour, K. M. (2009a). The involvement of H^+-ATPase and carbonic anhydrase in intestinal HCO_3^- secretion in seawater acclimated rainbow trout. *J. Exp. Biol.* **212**, 1940-1948.

Grosell, M., Mager, E. M., Williams, C. and Taylor, J. R. (2009b). High rates of HCO_3^- secretion and Cl^- absorption against adverse gradients in the marine teleost intestine: the involvement of an electrogenic anion exchanger and H^+-pump metabolon? *J. Exp. Biol.* **212**, 1684-1696.

Gross, E., Pushkin, A., Abuladze, N., Fedotoff, O. and Kurtz, I. (2002). Regulation of the sodium bicarbonate cotransporter kNBC1 function: role of Asp^{986}, Asp^{988} and kNBC1-carbonic anhydrase II binding. *J. Physiol.* **544**, 679-685.

Herrin, R. C. (1935). Chemical changes in blood and intestinal juice produced by the loss of intestinal juice. *J. Biol. Chem.* **108**, 547-562.

Hogan, D. L., Ainsworth, M. A. and Isenberg, J. I. (1994). Review article: gastroduodenal bicarbonate secretion. *Aliment. Pharmacol. Ther.* **8**, 475-488.

Horita, S., Yamada, H., Inatomi, J., Moriyama, N., Sekine, T., Igarashi, T., Endo, Y., Dasouki, M., Ekim, M., Al-Gazali, L., Shimadzu, M., Seki, G. and Fujita, T. (2005). Functional analysis of NBC1 mutants associated with proximal renal tubular acidosis and ocular abnormalities. *J. Am. Soc. Nephrol.* **16**, 2270-2278.

Jentsch, T. J., Schill, B. S., Schwartz, P., Matthes, H., Keller, S. K. and Wiederholt, M. (1985). Kidney epithelial cells of monkey origin (BSC-1) express a sodium bicarbonate cotransport. Characterization by $^{22}Na^+$ flux measurements. *J. Biol. Chem.* **260**, 15554-15560.

Kurita, Y., Nakada, T., Kato, A., Doi, H., Mistry, A. C., Chang, M., Romero, M. F. and Hirose, S. (2008). Identification of intestinal bicarbonate transporters involved in formation of carbonate precipitates to stimulate water absorption in marine teleost fish. *Am. J. Physiol. Regul. Integr. Comp. Physiol.* **294**, R1402-R1412.

Kyte, J. and Doolittle, R. F. (1982). A simple method for displaying the hydropathic character of a protein. *J. Mol. Biol.* **157**, 105-132.

Li, H. C., Li, E. Y., Neumeier, L., Conforti, L. and Soleimani, M. (2007). Identification of a novel signal in the cytoplasmic tail of the Na^+:HCO_3^- cotransporter NBC1 that mediates basolateral targeting. *Am. J. Physiol. Renal Physiol.* **292**, F1245-F1255.

Livak, K. J. and Schmittgen, T. D. (2001). Analysis of relative gene expression data using real-time quantitative PCR and the 2(-delta delta C(T)) method. *Methods* **25**, 402-408.

Lu, J. and Boron, W. F. (2007). Reversible and irreversible interactions of DIDS with the human electrogenic Na/HCO_3 cotransporter NBCe1-A: role of lysines in the KKMIK motif of TM5. *Am. J. Physiol. Cell Physiol.* **292**, C1787-C1798.

Lu, J., Daly, C. M., Parker, M. D., Gill, H. S., Piermarini, P. M., Pelletier, M. F. and Boron, W. F. (2006). Effect of human carbonic anhydrase II on the activity of the human electrogenic Na/HCO_3 cotransporter NBCe1-A in *Xenopus* oocytes. *J. Biol. Chem.* **281**, 19241-19250.

Marshall, W. S. and Grosell, M. (2006). Ion transport, osmoregulation and acid–base balance. In *The Physiology of Fishes* (ed. D. Evans and J. B. Claiborne), pp. 177-230. Boca Raton, FL: CRC.

McAlear, S. D., Liu, X., Williams, J. B., McNicholas-Bevensee, C. M. and Bevensee, M. O. (2006). Electrogenic Na/HCO_3 cotransporter (NBCe1) variants expressed in *Xenopus* oocytes: functional comparison and roles of the amino and carboxy termini. *J. Gen. Physiol.* **127**, 639-658.

McDonald, M. D., Grosell, M., Wood, C. M. and Walsh, P. J. (2003). Branchial and renal handling of urea in the gulf toadfish, *Opsanus beta*: the effect of exogenous urea loading. *Comp. Biochem. Physiol.* **134A**, 763-776.

McMurtrie, H. L., Cleary, H. J., Alvarez, B. V., Loiselle, F. B., Sterling, D., Morgan, P. E., Johnson, D. E. and Casey, J. R. (2004). Mini review: the bicarbonate transport metabolon. *J. Enzym. Inhib. Med. Chem.* **19**, 231-236.

Niv, Y. and Fraser, G. M. (2002). The alkaline tide phenomenon. *J. Clin. Gastroenterol.* **35**, 5-8.

Piermarini, P. M., Kim, E. Y. and Boron, W. F. (2007). Evidence against a direct interaction between intracellular carbonic anhydrase II and pure C-terminal domains of SLC4 bicarbonate transporters. *J. Biol. Chem.* **282**, 1409-1421.

Romero, M. F. and Boron, W. F. (1999). Electrogenic Na^+/HCO_3^- cotransporters: cloning and physiology. *Annu. Rev. Physiol.* **61**, 699-723.

Romero, M. F., Hediger, M. A., Boulpaep, E. L. and Boron, W. F. (1997). Expression cloning and characterization of a renal electrogenic Na^+/HCO_3^- cotransporter. *Nature* **387**, 409-413.

Romero, M. F., Fulton, C. M. and Boron, W. F. (2004). The SLC4 family of HCO_3^- transporters. *Pflügers Arch. – Eur. J. Physiol.* **447**, 495-509.

Sciortino, C. M. and Romero, M. F. (1999). Cation and voltage dependence of rat kidney, electrogenic Na^+/HCO_3^- cotransporter, rkNBC, expressed in oocytes. *Am. J. Physiol.* **277**, F611-F623.

Secor, S. M. (2009). Specific dynamic action: a review of the postprandial metabolic response. *J. Comp. Physiol. B*, **179**, 1-56.

Smith, H. W. (1930). The absorption and excretion of water and salts by marine teleosts. *Am. J. Physiol.* **93**, 480-505.

Sterling, D., Reithmeier, R. A. and Casey, F. R. (2001). A transport metabolon. Functional interaction of carbonic anhydrase II and chloride/bicarbonate exchangers. *J. Biol. Chem.* **276**, 47886-47894.

Taylor, J. R. and Grosell, M. (2006). Feeding and osmoregulation: dual function of the marine teleost intestine. *J. Exp. Biol.* **209**, 2939-2951.

Taylor, J. R. and Grosell, M. (2009). The intestinal response to feeding in seawater gulf toadfish, *Opsanus beta*, includes elevated base secretion and increased epithelial oxygen consumption. *J. Exp. Biol.* **212**, 3873-3881.

Taylor, J. R., Whittamore, J. M., Wilson, R. W. and Grosell, M. (2007). Postprandial acid–base balance and ion regulation in freshwater and seawater-acclimated European flounder, *Platichthys flesus*. *J. Comp. Physiol. B* **177**, 597-608.

Walsh, P. J., Blackwelder, P., Gill, K. A., Danulat, E. and Mommsen, T. P. (1991). Carbonate deposits in marine fish intestines: A new source of biomineralization. *Limnol. Oceanogr.* **36**, 1227-1232.

Wilson, R. W. (1999). A novel role for the gut of seawater teleosts in acid-base balance. In *Regulation of Acid-Base Status in Animals and Plants* (ed. S. Egginton, E. W. Taylor and J. A. Raven), pp. 257-274. Cambridge, UK: Cambridge University Press.

Wilson, R. W. and Grosell, M. (2003). Intestinal bicarbonate secretion in marine teleost fish – source of bicarbonate, pH sensitivity, and consequence for whole animal acid-base and divalent cation homeostasis. *Biochim. Biophys. Acta* **1618**, 163-193.

Wilson, R. W., Wilson, J. M. and Grosell, M. (2002). Intestinal bicarbonate secretion by marine teleost fish – why and how? *Biochim. Biophys. Acta* **1566**, 182-193.

Wood, C. M., Kajimura, M., Mommsen, T. P. and Walsh, P. J. (2005). Alkaline tide and nitrogen conservation after feeding in an elasmobranch (*Squalus acanthias*). *J. Exp. Biol.* **208**, 2693-2705.